JOURNAL OF MATERIALS SCIENCE 30 (1995) 4009–4013

Microstructural investigation of quartz submitted to ultra-short shock loading

P. CORDIER*, J. C. DOUKHAN
Laboratoire de Structure et Propriétés de l'Etat Solide-UA CNRS 234, Université des Sciences et Technologies de Lille, 59655 Villeneuve d'Ascq Cedex, France

A. MIGAULT, J. P. ROMAIN
Laboratoire d'Energétique et de Détonique-UA CNRS 193, Ecole Nationale Supérieure de Mécanique et d'Aérotechnique, BP 109–86960 Futuroscope Cedex, France

A high-energy pulsed laser was used to induce very short (2 ns) pressure pulses in quartz single crystals. The microstructure of recovered specimens was characterized by optical microscopy, scanning electron microscopy and transmission electron microscopy. Whatever the peak pressures (20–90 GPa), the shocked materials showed no shock defects (amorphous lamellae, Brazil twins, etc.). The microstructure was dominated by fracturing. The present study thus suggests that for very short pulse durations, quartz can be loaded at pressures well above the Hugoniot elastic limit without undergoing solid-state amorphization. The behaviour of quartz is purely elastic–brittle.

1. Introduction

The mechanical response of minerals submitted to shock waves has recently attracted considerable attention. Indeed, meteorite impacts now appear as a major geological process with possible implications on the formation of the Earth and the evolution of the biota. As meteorite impact craters on the Earth's surface are often very eroded, shock metamorphism (i.e. the microstructural signature left by a shock wave in silicates) usually represents the main source of information on the impact event. So there is a need for a better understanding of the mechanical behaviour of silicates under shock. Experimental studies on shock metamorphism are most often performed by dynamic methods, for instance by impacts of metal plates accelerated by a light gas gun or by high explosives [1]. Pressures up to 100 GPa can be generated by these methods with pulse durations of the order of 1 μs (using reverberations of the shock wave in the target). For comparison, meteorite impacts correspond to shock durations of 1 ms up to ≈1 s for the largest bolides. The importance of the shock intensity is largely recognized as an important parameter for the formation of the shock-induced defect microstructure. However, the time duration of the shock pulse may also be a relevant parameter and it is important to investigate its possible influence. The availability of powerful pulsed lasers provides a new experimental tool to generate very high dynamic pressures [2] during very short times (order of nanoseconds). This new tool provides an opportunity to investigate the kinetics of high-pressure microstructural modifications under shock.

The present study focuses on quartz as a target. The ubiquity and abundance of quartz in the Earth's continental crust makes it a good indicator of shock metamorphism in impact craters. A large number of studies have been recently performed on quartz. Both naturally shocked specimens from impact craters [3] and samples experimentally shocked using light-gas guns or high explosives were investigated [4–9], see also a review in [1]). The most widespread signature of a shock wave in quartz is the formation of straight and narrow amorphous lamellae parallel to a few specific crystallographic planes. Amorphization of quartz under pressure has been extensively studied in the last few years, both theoretically and experimentally (under shock and statically in diamond anvil cells). The present study, based on ultra-short shock loading of quartz, aimed to address the question of the amorphization kinetics under shock. Real-time measurements have already yielded some information on laser-shocked quartz [10]. In the present work, we use the complementary approach of microstructural characterizations on recovered samples using scanning electron microscopy (SEM), optical microscopy (OM) and transmission electron microscopy (TEM).

2. Experimental procedure

The experiments were conducted at the LULI (Laboratoire pour l'Utilisation des Lasers Intenses, Ecole

* Author to whom all correspondence should be addressed.

0022–2461

TABLE I Experimental conditions used in this study

Run	Laser energy (J)	Focal spot (mm)	Incident flux (10^{12} W cm^{-2})	Induced pressure P_i (GPa)
1	80	2.6	622	34
2	80	2.6	622	34
3	80	2.6	622	34
4	80	2.6	622	34
5	80	2.6	622	34
6	100	1	4740	144
7	45	1	2230	84
8	85	1	4070	130

TABLE II Numerical values for quartz used in the simulation

Density	2.65 g cm^{-2}
Gruneisen parameter	0.7
Bulk modulus	37.7 GPa
Bulk sound velocity	3.77 mm μs^{-1}
Poisson's ratio	0.215
Hugoniot elastic limit	6 GPa

Polytechnique, Palaiseau, France) with a neodynium–glass laser. The laser wavelength was 1.06 μm, the pulse duration at half-maximum was 2 ns and the focal spot was adjusted (between 2.5 and 1 mm) so as to generate peak pressures in the range 30–140 GPa.

Parallelepiped (typically 1.5 cm × 1.5 cm × 1.5 cm in size) single crystals of synthetic quartz were used for this study. The irradiated surface was first optically polished. A 25 μm aluminium film covered with a black paint layer was then deposited on to the surface. The specimens were shocked along the X direction (a = 1/3 [$\bar{2}$ 1 1 0]).

The pressure, P_i, induced in the target by the laser pulse has been estimated from scaling laws deduced from previous experimental results and relating the pressure to laser energy, diameter of the focal spot, and pulse duration at half-maximum. The values reported in Table I represent an average of these various results [11–14]. The accuracy can be estimated at ± 20%.

Shock attenuation during the propagation through the target is computed with a hydrodynamic Lagrangian code (SHYLAC) including an equation of state and a constitutive law for the material [15]. Simulations are made on X-cut quartz samples identical to those used for experiments. The required parameters at zero pressure are taken from Swegle [16] ; they are displayed in Table II. The Hugoniot curve is also taken from Swegle [16]; this curve is represented by a fourth-order polynomial of the variable (V_0/V − 1). In this representation, we have taken the coefficient of the first term equal to K_0 as predicted theoretically. Calculations were made for three induced pressures, P_i = 34, 84 and 130 GPa. The results show that the peak pressure remains above 10 GPa (i.e. above the Hugoniot elastic limit of quartz) for 25, 65 and 115 ns, respectively. The corresponding depths are 140, 400 and 700 μm respectively, see Fig. 1.

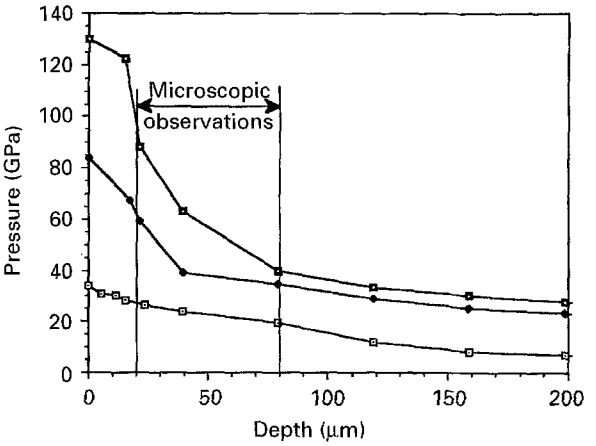

Figure 1 Attenuation profile of the shock wave below the irradiated surface calculated with the SHYLAC code. Three induced pressures have been considered here: (□) 34, (◆) 84 and (■) 130 GPa. The depth range of the microscopic observations presented in this study is emphasized.

3. Microscopic observations

3.1. Crater morphology

The morphology of the craters formed by the laser pulses has been studied using OM with reflected light and SEM which has a larger depth of focus and thus allows the whole crater to be seen at once. Fig. 2a shows a scanning electron micrograph of a sample from run 5. The crater has approximately the size of the focal spot used for the laser-shock experiment. However, it is clear from this micrograph (especially in the upper right corner) that chipping occurred, resulting in a slightly larger crater. At higher magnification (Fig. 2b) the bottom of the crater appears to be dominated by surface steps, the so-called "Wallner" lines, typical of brittle fracture. OM with reflected light was used to measure crater depths. Maximal depths were found to lie between 50 and 80 μm for all experiments. In some cases some fragments remained attached to the surface. A fracture sub-parallel to the surface, underlying those fragments, was systematically revealed by OM observations with reflected light.

3.2. Microstructural investigation (OM and TEM)

Thin foils were cut in the shocked samples in order to investigate the shock-induced defect microstructures.

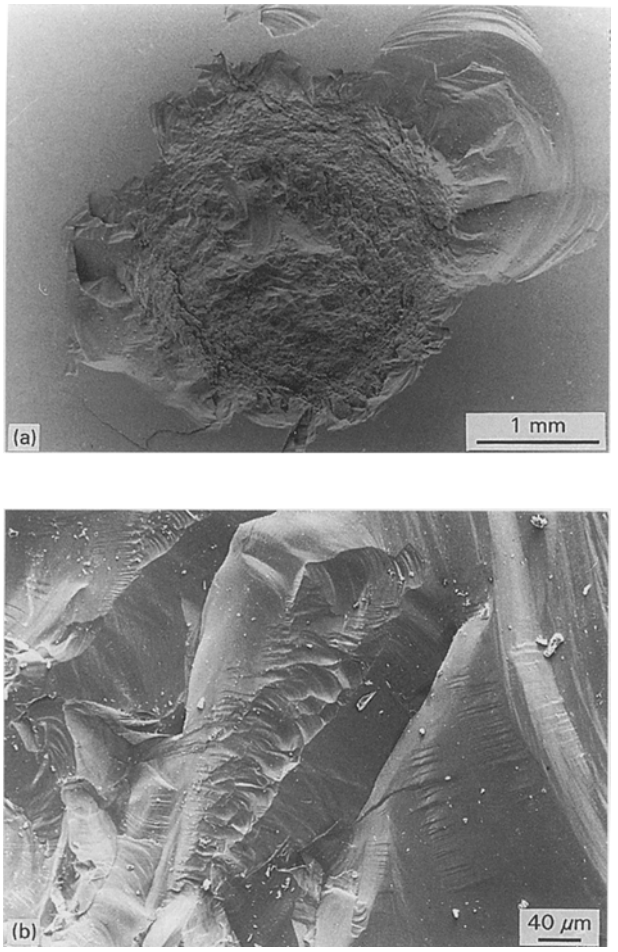

Figure 2 Scanning electron micrographs of laser-induced craters. (a) General view, experiment 5, $P_i = 34$ GPa. (b) Experiment 3, $P_i = 34$ GPa: larger magnification; note the hackle morphology.

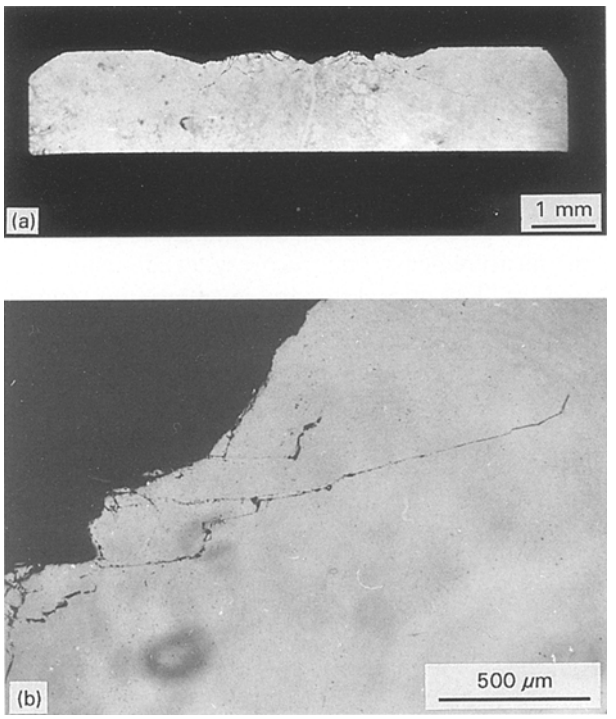

Figure 3 Experiment 5, $P_i = 34$ GPa. Optical micrograph, transmitted light, crossed polarizers. Thin foil cut perpendicular to the irradiated surface (cross-section). (a) General view showing the crater profile. (b) Enlargement of the right side of (a) showing the cracks running below the surface.

Two orientations were selected for that purpose. The first one parallel to the irradiated surface was cut at the level of the bottom of the crater in order to have an overview of the microstructure just below this crater. The information collected by both OM and TEM stems from regions located at 10–20 μm below the bottom of the crater, i.e. at ≈100 μm below the original surface. The second orientation was chosen perpendicular to the first one (cross-section) running through the middle of the crater. Given the irregular profile of the crater (see Fig. 3a), this orientation gave the opportunity to investigate the microstructure at very shallow depths: 20–30 μm from the original irradiated surface.

In OM the first types of thin foils (parallel to the irradiated surface) show below the crater a dense network of cracks. These cracks are not straight and their orientations do not seem to be strongly crystallographically controlled. These thin specimens show sharp extinctions between cross polarizers. No defects or strain are detected between the cracks by OM. Fig. 3b is a typical optical micrograph for the second type of thin section (cross-section) corresponding to experiment 5. One can see the cracks below the crater. The longer cracks are nucleated at the rim of the crater and extend in a cone very similar to those observed in the case of Hertzian cracking. Once again, no defects are detected between cracks.

TEM investigations were performed on specimens from runs 2, 3, 5, 7 and 8. The microstructures are similar in all of them. None of the usual shock-induced lattice defects were detected. Neither were any dislocations, mechanical twin lamellae or amorphous patchs detected. The observed microstructures are dominated by a pervasive network of microcracks at any scale (Fig. 4). In the TEM, microcracks appear as curviplanar defects exhibiting Moiré patterns which reflect slight variations of the free surfaces of the cracks. Between the cracks, quartz is pristine.

4. Discussion and conclusion

The salient point emerging from this study is the observation at any stage of the investigation of a pervasive evidence of brittleness under laser-induced shocks. The first evidence is from the topography of the crater with its irregular and very sharp profile. No evidence of plastic flow, amorphization or melting is detected. On the contrary, well-developed parallel surface steps characteristic of brittle tensile failure are observed.

Optical examination of the cracks formed by the shock pulses, on both the bulk specimens and the cross-sections, indicate that cone-shaped cracks were formed. Such cone fractures are well known in fracture mechanics of brittle materials as arising from Hertzian cracking. Usually, the Hertzian contact results from the contact of an elastic sphere (the indentor) pressed on to a flat specimen. The cone fracture which extends in the Hertzian field is characteristic of a specimen with a purely elastic behaviour until brittle fracture occurs (see, for instance, [17]).

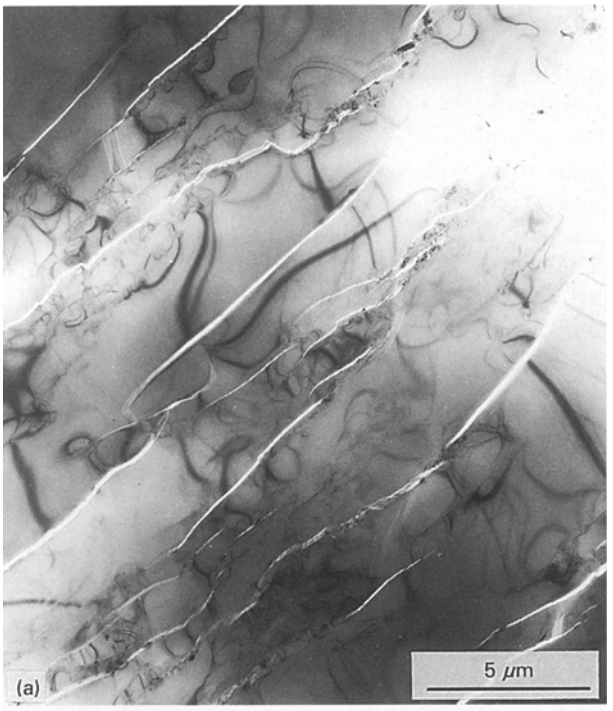

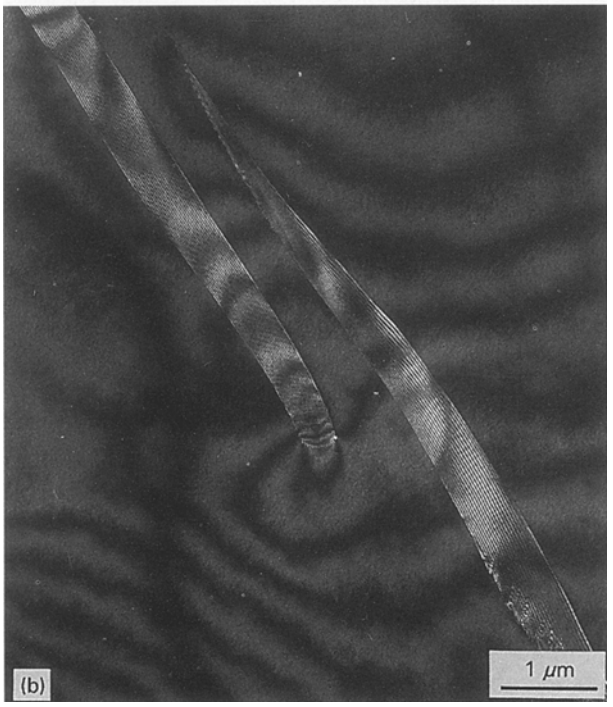

Figure 4 Transmission electron micrographs: (a) experiment 7, $P_i = 84$ GPa, bright field showing the numerous open fractures; (b) experiment 2, $P_i = 34$ GPa, weak-beam micrograph showing the microcracks (evidenced by their Moiré pattern) in a pristine matrix.

Purely brittle behaviour is finally indicated by our TEM observations. Indeed, even at crack tips where the stress must have reached quite high levels, we observe no crack blunting by dislocation emission. We wish to emphasize here that, given the strong attenuation of the laser-induced shock wave, we paid a great attention to the material at very shallow depths. Simulations reported in Fig. 1 show that our TEM observations were performed in regions where the pressure ranges from 20–90 GPa. This complete absence of ductility under shock in quartz is not surprising, and has already been demonstrated by shock-gun experiments [4]. Moreover, detailed microscopic studies on recovered specimens from laboratory experiments has led to a good calibration of shock effects in quartz as a function of pressure and temperature (see [1] for a recent review). Above 5–7 GPa, shocked quartz exhibits planar fractures parallel to rational low-index planes: (0 0 0 1) and $\{1\,0\,\bar{1}\,1\}$ mostly. This is already indicative of shock, because quartz has, in normal conditions (i.e. at room pressure), no cleavage planes. Planar deformation features (PDFs) are formed for pressures exceeding 10 GPa. These PDFs are amorphous lamellae lying in some rational low-index planes: $\{1\,0\,\bar{1}\,n\}$ ($n = 2, 3, 4$) and $\{1\,1\,\bar{2}\,2\}$. Mechanical twins in the basal plane also form in these conditions. Diaplectic quartz glass is found in quartz samples submitted to peak pressures in the range 35–50 GPa. Above 50 GPa, the occurrence of Lechatelierite (fused silica quenched to silica glass) shows that quartz melted, at least partially. Vaporization is thought to occur above 60 GPa. Given this scale, it could be surprising that no shock-induced defects are nucleated in our specimens. It should be remembered, however, that the above calibration stems from specimens experimentally shocked with high explosives or light-gas guns which correspond to much longer pressure durations than in the present study. Our present study suggests that quartz can be loaded at pressures well above the Hugoniot elastic limit without undergoing any transformation, other than fracturing, if the pressure pulse duration is short enough. In particular, the solid-state amorphization (PDF) which occurs for pressures above 10 GPa was inhibited in our experiments. This observation should be compared with the time-resolved measurements of Ng *et al.* [10] on shock-loaded quartz. These authors measured the shock trajectory and showed that the double-wave structure characteristic of the mixed-phase regime of the Hugoniot curve was not clearly apparent. The Hugoniot data they deduced from experiments performed in the range 50–300 GPa, are significantly above the so-called equilibrium Hugoniot. Both real-time measurements and recovery experiments followed by TEM microstructural investigations suggest that the occurrence of the dense amorphous silica, which is characteristic of the mixed-phase regime of the Hugoniot, cannot be nucleated by pulse durations as short as 2 ns. However, Ng *et al.* suggested that, under laser-shock conditions, quartz might transform at the shock front into a disordered phase before relaxing to stishovite. Our microstructural investigations do not support this hypothesis at least in the pressure range investigated here. On the one hand, we observe in the final state no transformation to stishovite or any (amorphous for instance) denser phase. On the other hand, it seems unlikely that quartz could transform into a disordered state and then revert to the perfectly pristine material observed by TEM between the microcracks. The pervasive evidence of such microcracks rather suggests that quartz exhibits a purely elastic–brittle behaviour under laser-shocks.

Acknowledgements

We thank Michel Boustie and the team of the LULI for their help during the laser shock experiments, and Stéphane Couturier and Thibaut de Resseguier for help with the simulations. Jean Michel Gloaguen provided assistance for the SEM investigations. Finally we thank Andrey Zhuk for fruitful discussions. This work was supported by DRED (ATF "Changements de phases à cinétiques très rapides sous pressions statiques et dynamiques").

References

1. D. STÖFFLER and F. LANGENHORST, *Meteoritics* **29** (1994) 155.
2. TH. LÖWER and R. SIGEL, *Contr. Plasma Phys.* **33** (1993) 355.
3. O. GOLTRANT, H. LEROUX, J. C. DOUKHAN and P. CORDIER, *Phys. Earth Planet Interiors* **74** (1992) 219.
4. A. J. GRATZ, *J. Non-Cryst. Solids* **67** (1984) 543.
5. A. J. GRATZ, J. TYBURCZY, J. CHRISTIE, T. AHRENS and P. PONGRATZ, *Phys. Chem. Mineral.* **16** (1988) 221.
6. A. J. GRATZ, W. J. NELLIS, J. M. CHRISTIE, W. BROCIOUS, J. SWEGLE and P. CORDIER, *ibid.* **19** (1992) 267.
7. A. R. HUFFMANN, J. M. BROWN, N. L. CARTER and W. U. REIMOLD, *J. Geophys. Res.* **98** (1993) 22171.
8. F. LANGENHORST, A. DEUTSCH, D. STÖFFLER and U. HORNEMANN, *Nature* **356** (1992) 507.
9. F. LANGENHORST and A. DEUTSCH, *Earth Planet. Sci. Lett.* **125** (1994) 407.
10. A. NG, B. K. GODWAL, J. WATERMAN, L. DASILVA, N. W. ASHCROFT and R. JEANLOZ, *Phys. Rev. B* **44** (1991) 4872.
11. B. STEVERING and P. DUDEL, *J. Appl. Phys.* **47** (1976) 1940.
12. C. R. PHILIPPS Jr, T. P. TURNER, R. F. HARISON, G. W. YORK, W. Z. OSBORNE, G. K. ANDERSON, X. F. CORLIS, L. C. HAYNES, H. S. STEELE, K. C. SPICOCHI and T.R. KING, *ibid.* **64** (1988) 1023.
13. R. FABBRO, J. FOURNIER, P. BALLARD, D. DEVAUX and J. VIRMONT, *ibid.* **68** (1990) 775.
14. J. GRUN, R. DECOSTE, B. H. RIPIN and J. GARDNER, *Appl. Phys. Lett.* **39** (1981) 545.
15. F. COTTET and M. BOUSTIE, *J Appl. Phys.* **66** (1989) 4067.
16. J. W. SWEGLE, *ibid.* **68** (1990) 1563.
17. B. R. LAWN and R. WILSHAW, *J. Mater. Sci.* **10** (1975) 1049.

Received 14 November 1994
and accepted 5 April 1995